2D Semiconductors Hot Paper

DOI: 10.1002/anie.201411246

Atomically Thin Arsenene and Antimonene: Semimetal–Semiconductor and Indirect–Direct Band-Gap Transitions**

Shengli Zhang, Zhong Yan, Yafei Li, Zhongfang Chen, and Haibo Zeng**

Abstract: *The typical two-dimensional (2D) semiconductors MoS_2, $MoSe_2$, WS_2, WSe_2 and black phosphorus have garnered tremendous interest for their unique electronic, optical, and chemical properties. However, all 2D semiconductors reported thus far feature band gaps that are smaller than 2.0 eV, which has greatly restricted their applications, especially in optoelectronic devices with photoresponse in the blue and UV range. Novel 2D mono-elemental semiconductors, namely monolayered arsenene and antimonene, with wide band gaps and high stability were now developed based on first-principles calculations. Interestingly, although As and Sb are typically semimetals in the bulk, they are transformed into indirect semiconductors with band gaps of 2.49 and 2.28 eV when thinned to one atomic layer. Significantly, under small biaxial strain, these materials were transformed from indirect into direct band-gap semiconductors. Such dramatic changes in the electronic structure could pave the way for transistors with high on/off ratios, optoelectronic devices working under blue or UV light, and mechanical sensors based on new 2D crystals.*

Two-dimensional (2D) crystals have rather unique and exceptional properties and promising applications. Typically, graphene permits electrons to flow freely across its surfaces, resulting in excellent electron mobility, which enables its superior performance in transistors and as electrochemical electrodes.[1] However, the Achilles' heel of the electronic structure of graphene, and also of silicene and germanene, is the zero band gap,[2] which seriously reduces their ability to switch current on and off in transistors, even though with surface functionalization and external electric or strain fields, very small band gaps can be achieved.[3] Considering their photoresponse, the identification of 2D semiconductors with different band-gap energies for applications in optoelectronic devices is of utmost importance.

Recently, several typical 2D semiconductors, namely monolayers of MoS_2, $MoSe_2$, WS_2, and WSe_2 as well as few-layered black phosphorus, were successfully fabricated.[4] Such extreme thinning indeed results in substantial changes in their electronic structures and hence in new optoelectronic properties and applications in devices.[5] For example, unlike bulk MoS_2 with its indirect band gap, monolayer MoS_2 was found to be a direct band gap semiconductor and thus displays much stronger luminescence. However, the band gaps of most explored 2D materials are smaller than 2.0 eV, which has greatly impeded the development of 2D semiconductor based optoelectronic devices with response to photons with wavelengths of less than 620 nm, such as blue- and UV-light-emitting diodes (LEDs) and photodetectors.

Herein, we identified two novel 2D wide-band-gap semiconductors with high stabilities, namely arsenene (As monolayer) and antimonene (Sb monolayer), by means of density functional theory (DFT) calculations. The bulk-to-monolayer transition is accompanied by an abrupt switch in the electronic properties from semimetallic to semiconducting. Free-standing arsenene and antimonene are indirect band-gap semiconductors (with band gaps of 2.49 and 2.28 eV, respectively). Interestingly, they can be converted into direct band-gap semiconductors under biaxial strain, which implies that aside from promising electronic and optoelectronic properties, these novel 2D semiconductors can also be anticipated to function as mechanical sensors.

Bulk As and Sb have many allotropes (Supporting Information, Table S1), and their layered structures are stable under ambient conditions.[6] These layered models were optimized by periodic DFT calculations. The relaxed As and Sb systems have similar structures, thus we take the model of layered gray As to describe both of their structures. The other relaxed structures are shown Table S2.

Structural models of As in the bulk and of its monolayer are shown in Figure 1; they share some features with graphite and graphene, for example, the honeycomb lattice. However, the arsenene layers adopt buckled structures to increase their stability (see below; thickness of the arsenene layer: 1.35 Å). For As in the bulk, interlayer distances, bond lengths, and

[*] Dr. S. Zhang, Prof. Z. Yan, Prof. H. Zeng
Institute of Optoelectronics & Nanomaterials
Herbert Gleiter Institute of Nanoscience
College of Materials Science and Engineering
Nanjing University of Science and Technology
Nanjing, 210094 (China)
E-mail: zeng.haibo@njust.edu.cn
Prof. Dr. Y. Li
College of Chemistry and Materials Science
Jiangsu Key Laboratory of Biofunctional Materials
Nanjing Normal University
Nanjing, 210023 (China)
Prof. Dr. Z. Chen
Department of Chemistry, Institute for Functional Nanomaterials
University of Puerto Rico
Rio Piedras, San Juan, PR 00931 (USA)
E-mail: zhongfangchen@gmail.com

[**] This work was financially supported by the National Basic Research Program of China (2014CB931700), the NSFC (61222403, 21403109, and 21403115), the NSF of Jiangsu Province (BK20140769), and in the USA by the Department of Defense (W911NF-12-1-0083). We also acknowledge the Computer Network Information Center (Supercomputing center) of the Chinese Academy of Sciences and the National Supercomputing Center in Shenzhen for providing computing resources.

Supporting information for this article is available on the WWW under http://dx.doi.org/10.1002/anie.201411246.

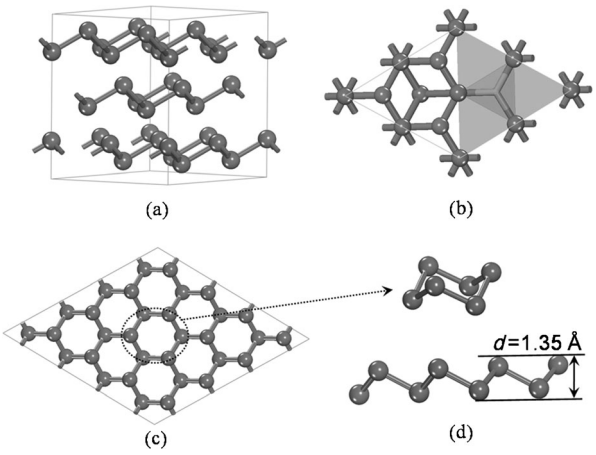

Figure 1. a) Side view and b) top view of the structure of gray arsenic. c) Top view and d) side view of a wrinkling As monolayer (arsenene).

bond angles of 2.04 Å, 2.49 Å, and 97.27°, respectively, were determined. In comparison, in arsenene, owing to the lattice distortion, the corresponding bond lengths and angles are 2.45 Å and 92.54°, respectively. Similarly distorted bond lengths and angles were also found in antimonene (Table S2).

Stability and experimental feasibility are important properties of new 2D crystals. We thus examined the phonon spectra, the configurational stability of the octet, the interlayer interaction forces, and possible epitaxial growth methods. Phonon calculations, reflecting soft modes, provide a criterion to judge the structure instability.[7] No soft phonon modes are available in the computed phonon dispersion spectra of arsenene and antimonene (Figure 2),

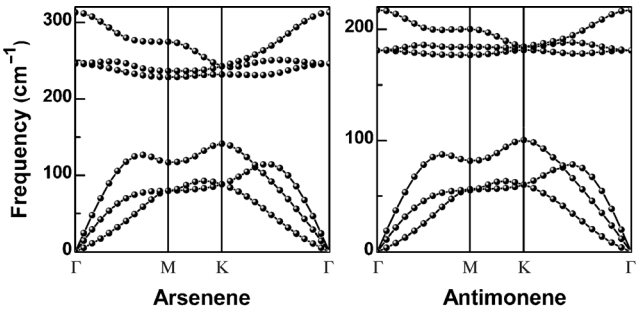

Figure 2. Phonon band dispersions of wrinkling arsenene and antimonene, which exhibit outstanding kinetic stability.

which demonstrates that arsenene and antimonene are kinetically very stable. Furthermore, each As or Sb atom (with five valence electrons) is bonded to three adjacent atoms in the same monolayer, which endows them with octet stability. The buckled honeycomb structure, similar to those of buckled silicene and germanene,[8] also helps stabilize the layered structure. Importantly, the interlayer interaction energies of layered As and Sb (89.6 and 86.0 meV per atom, respectively, by DFT calculations with the Grimme van der Waals correction)[9] are very close to that of graphite (computed: 63.5 meV per atom; experimental: 63 meV per atom). Considering the successful fabrication of graphene by exfoliation and growth on SiC or metal surfaces,[10] the syntheses of arsenene and antimonene by similar methods should be feasible.

We then examined the variation of the electronic band structure of As upon reducing the layer numbers (Figure S1 and Figure 3). Gray As preserves its metallic character when

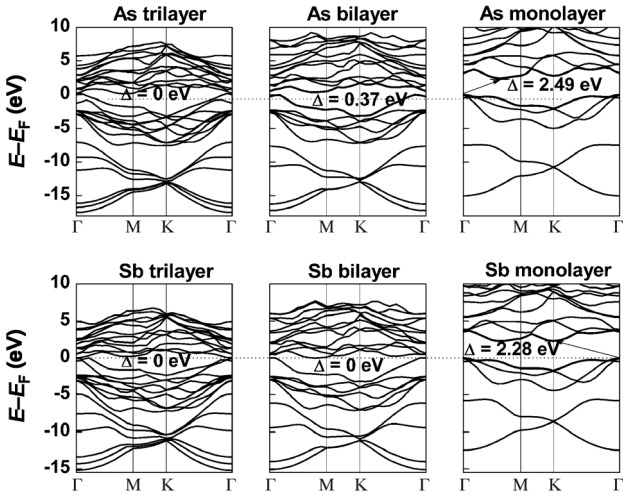

Figure 3. Electronic band structures of arsenic and antimony trilayers and bilayers and their monolayers (arsenene and antimonene) calculated at the HSE06 level of theory. •••••: Fermi levels.

a bulk sample is thinned to a trilayer. The metallic character of multilayered As is mainly due to the fact that the 4p orbitals cross the Fermi level at several points in the Brillouin zone. A significant change occurs when the thickness is decreased to a bilayer, and a small but clear band gap of 0.37 eV was calculated (Figure 3). The valence-band top and the conduction-band bottom of the As bilayer mainly consist of As 4p states. Most importantly, an abrupt transition from semimetallic or metallic As multilayers to a semiconducting arsenene structure with a band gap of 2.49 eV was observed. These results demonstrate that a new band gap has been formed in arsenene; therefore, the As material has been transformed into a 2D wide-band-gap semiconductor.

Similar electronic structure transitions from a metal to a semiconductor were also observed when Sb was thinned to a monolayer (Figure S2 and Figure 3). Sb trilayers and bilayers are metallic with the valence-band top and the conduction-band bottom crossing the Fermi level at several points in the Brillouin zone. However, for monolayered antimonene, the valence band shifts down slightly while the conduction band shifts up significantly, resulting in a persistent decrease of the overlapping zone of the two bands and thus in the formation of a 2.28 eV band gap. Therefore, the free-standing antimonene monolayer is also an indirect semiconductor with a wide band gap.

Our above computations show that only monolayered arsenene and antimonene feature a wide band gap. To understand the intrinsic mechanism for its formation we need to consider two aspects.

First, second-order effects play an important role.[11] Within the layered system, the As and Sb atoms with lone-pair electrons are situated alternately in an upper and a lower plane, which results in significant puckering and a pseudo-Jahn–Teller distortion. The interlayer interactions are present from the multilayer all the way to the bilayer (see Figure S3). Our computations (Figure S4) show that the interlayer interactions for As/Sb systems with six to two layers are in the range of 0.12–0.24 eV per unit and decrease with an increase in layer thickness. Thus, we believe that the dependence of the interlayer interaction on the layer thickness most likely plays an important role in the semimetal to wide-band-gap semiconductor transition in the As/Sb layered systems.

The quantum confinement effect is the second main factor effecting the electronic structure transition. When the thickness of the originally semimetallic or metallic film is reduced to a monolayer, the conduction bands of the As/Sb monolayer shift towards the vacuum level (Figure 3). In arsenene and antimonene, the conduction-band bottom mainly consists of As 4p (Sb 5p) states coupled with small amounts of 4s (Sb 5s) states; six As 4p (Sb 5p) states split into three bonding and three antibonding states forming a band gap around the Fermi level.

To gain further insights, we also computed the density of states and the electron density isosurfaces for both the valence band maximum (VBM) and the conduction band minimum (CBM) of the arsenene and antimonene monolayers (Figures S5 and S6). Both the VBMs and CBMs of arsenene and antimonene are combinations of mainly p atomic orbitals. With their buckled and layered structures, arsenene and antimonene are structurally similar to silicene and germanene; however, their electronic properties differ significantly. In semimetallic silicene and germanene, the valence-band top and conduction-band bottom consist of π-type bonding states;[12] in contrast, in arsenene and antimonene, there are three σ-bonding orbitals and a lone pair of electrons, which decline to form π-type bonding states. This is probably the underlying reason for the different electronic properties of silicene and germanene in Group 4 and arsenene and antimonene in Group 5.

However, when used in optoelectronic devices, both arsenene and antimonene will suffer from poorly efficient light emission owing to the indirect band gaps. Encouragingly, we found that both arsenene and antimonene experience an intriguing indirect-to-direct band-gap transition at a relatively small critical strain. In Figure 4, we present the changes in the electronic band structures upon applying a biaxial tensile strain to arsenene (for details, see Figure S7 and S8). Under 0–3% tensile strain, the CBM of monolayered arsenene remains in the Brillouin zone halfway between the Γ and M high-symmetry points (Figure 4a). However, further increasing the strain up to 4% shifts the CBM to the Γ high-symmetry point, which rapidly transforms arsenene into a direct band-gap semiconductor. This direct band gap persists under a tensile strain of 4 to 12% (Figure 4b and c). The overall trends in the changes of the electronic-band character of monolayered antimonene in response to biaxial tensile strain (Figure S8) are quite similar to those for arsenene. The direct band structure of the strained monolayers has a clear advantage for their applications in optical devices, as electronic excitation is now feasible with lower phonon energies. It is noteworthy that strain effects have been suggested, both experimentally and theoretically, as an effective way to tune electronic properties, for example, an indirect band gap.[13] Moreover, 2D materials can endure a great tensile strain, which can be realized experimentally by a lattice mismatch on the substrate or mechanical loading.[14]

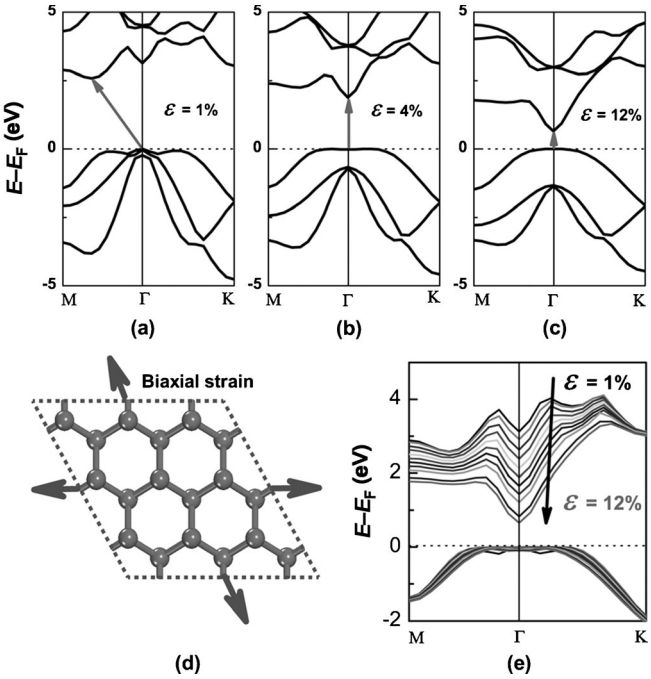

Figure 4. a–c) Electronic band structures of arsenene under 1% (a), 4% (b), and 12% (c) biaxial strain calculated at the HSE06 level of theory. d) Schematic representation of arsenene under biaxial tensile strain. e) Changes in the valence-band top and the conduction-band bottom with increasing biaxial tensile strain.

We also computed the effective mass of the electron according to the valence bands of arsenene and antimonene at the Γ point along the Γ–K and the Γ–M directions. For arsenene, the effective electron masses were computed to be $m_e^{\Gamma K} = 0.23\,m_o$ and $m_e^{\Gamma M} = 0.29\,m_o$, and for the antimonene monolayer, the effective electron masses were found to be $m_e^{\Gamma K} = 0.20\,m_o$ and $m_e^{\Gamma M} = 0.24\,m_o$ (all masses calculated with the HSE06 hybrid functional; m_o is the free-electron mass). These values are close to that of black phosphorene ($m_e^{\Gamma X} = 0.17\,m_o$), but smaller than those of monolayer black phosphorene ($m_e^{\Gamma Y} = 1.12\,m_o$) and monolayer MoS_2 ($m_e = 0.48\,m_o$).[15] It is likely that arsenene and antimonene, similar to black phosphorus, will exhibit a higher carrier mobility than monolayer MoS_2. Their outstanding properties, including small effective carrier masses, increased mobilities, and wide direct band gaps, should render these materials suitable for future applications in high-speed ultrathin transistors and in blue LEDs and photodetectors.

In conclusion, we have reported two-dimensional semiconducting arsenene and antimonene sheets with distinguished structures and properties. An abrupt transition from semimetallic or metallic As and Sb multilayers to wide-band-

gap semiconductor arsenene and antimonene monolayers was observed. Our calculated band structures indicate that monolayered arsenene and antimonene are indirect semiconductors with wide band gaps of 2.49 and 2.28 eV, respectively. More interestingly, both arsenene and antimonene undergo an indirect-to-direct band-gap transition upon tensile strain; therefore, they are promising materials for applications in optoelectronics. Semiconductor materials of Group 5 elements were reported for the first time, and feasible wide-band-gap semiconductors for experimental realization and materials for nanoelectronic and optoelectronic devices have been identified. We believe that these novel materials will be synthesized in the laboratory in the very near future.

Experimental Section

All calculations were performed using the plane wave code CASTEP[16] under the general gradient approximation (GGA) expressed by the PBE functional.[17] To describe the interlayer van der Waals interactions, we used the PBE functional with the Grimme dispersion correction.[18] All of the structure models were fully relaxed, including the cells of As and Sb, until the forces were smaller than 0.01 eV Å^{-1} and the energy tolerances less than 5×10^{-6} eV per atom. A vacuum of 15 Å between these 2D layered structures was used with $13\times13\times3$ Monkhorst–Pack k-points and a plane-wave cutoff energy of 550 eV. The band structures were evaluated by both PBE and the screened hybrid functional, HSE06, which typically gives a better description of band gaps in semiconductors.[19]

Received: November 20, 2014
Published online: January 7, 2015

Keywords: antimony · arsenic · density functional calculations · electronic properties · semiconductors

[1] S. Das Sarma, S. Adam, E. H. Hwang, E. Rossi, *Rev. Mod. Phys.* **2011**, *83*, 407.
[2] Y. Pan, L. Z. Zhang, L. Huang, L. F. Li, L. Meng, M. Gao, Q. Huan, X. Lin, Y. L. Wang, S. X. Du, H. Freund, H. J. Gao, *Small* **2014**, *10*, 2215.
[3] a) Y. Zhang, T. T. Tang, C. Girit, Z. Hao, M. C. Martin, A. Zettl, M. F. Crommie, Y. R. Shen, F. Wang, *Nature* **2009**, *459*, 820; b) X. Li, X. Wang, L. Zhang, S. Lee, H. Dai, *Science* **2008**, *319*, 1229; c) Q. Tang, J. Bao, Y. F. Li, Z. Zhou, Z. F. Chen, *Nanoscale* **2014**, *6*, 8624; d) Y. Jing, Z. Zhou, C. R. Cabrera, Z. F. Chen, *J. Mater. Chem. A* **2014**, *2*, 12104.
[4] a) L. K. Li, Y. J. Yu, G. J. Ye, Q. Q. Ge, X. D. Ou, H. Wu, D. L. Feng, X. H. Chen, Y. B. Zhang, *Nat. Nanotechnol.* **2014**, *9*, 372; b) X. D. Zhang, Y. Xie, *Chem. Soc. Rev.* **2013**, *42*, 8187.
[5] a) X. F. Song, H. B. Zeng, *J. Mater. Chem. C* **2013**, *1*, 2952; b) Q. Tang, Z. Zhou, *Prog. Mater. Sci.* **2013**, *58*, 1244; c) H. B. Zeng, C. Y. Zhi, Z. H. Zhang, X. L. Wei, X. B. Wang, W. L. Guo, Y. Bando, D. Golberg, *Nano Lett.* **2010**, *10*, 5049.
[6] N. C. Norman, *Chemistry of Arsenic, Antimony and Bismuth*, Academic Press, Springer, **1998**.
[7] Y. F. Li, Y. L. Liao, Z. F. Chen, *Angew. Chem. Int. Ed.* **2014**, *53*, 7248; *Angew. Chem.* **2014**, *126*, 7376.
[8] S. Cahangirov, M. Topsakal, E. Aktük, H. Sahin, S. Ciraci, *Phys. Rev. Lett.* **2009**, *102*, 236804.
[9] R. Zacharia, H. Ulbricht, T. Hertel, *Phys. Rev. B* **2004**, *69*, 155406.
[10] a) L. Chen, Y. Hernandez, X. L. Feng, K. Müllen, *Angew. Chem. Int. Ed.* **2012**, *51*, 7640; *Angew. Chem.* **2012**, *124*, 7758; b) C. N. R. Rao, A. K. Sood, K. S. Subrahmanyam, A. Govindaraj, *Angew. Chem. Int. Ed.* **2009**, *48*, 7752; *Angew. Chem.* **2009**, *121*, 7890.
[11] a) R. G. Pearson, *Proc. Natl. Acad. Sci. USA* **1975**, *72*, 2104; b) T. Hughbanks, R. Hoffmann, *J. Am. Chem. Soc.* **1983**, *105*, 3528.
[12] P. Vogt, P. De Padova, C. Quaresima, J. Avila, E. Frantzeskakis, M. C. Asensio, A. Resta, B. Ealet, G. Le Lay, *Phys. Rev. Lett.* **2012**, *108*, 155501.
[13] a) J. Feng, X. F. Qian, C. W. Huang, J. Li, *Nat. Photonics* **2012**, *6*, 865; b) K. He, C. Poole, K. F. Mak, J. Shan, *Nano Lett.* **2013**, *13*, 2931; c) P. Miró, M. Ghorbani-Asl, T. Heine, *Angew. Chem. Int. Ed.* **2014**, *53*, 3015; *Angew. Chem.* **2014**, *126*, 3059.
[14] H. Shi, H. Pan, Y.-W. Zhang, B. I. Yakobson, *Phys. Rev. B* **2013**, *87*, 155304.
[15] J. S. Qiao, X. H. Kong, Z. X. Hu, F. Yang, W. Ji, *Nat. Commun.* **2014**, *5*, 4475.
[16] M. D. Segall, P. J. D. Lindan, M. J. Probert, C. J. Pickard, P. J. Hasnip, S. J. Clark, M. C. Payne, *J. Phys. Condens. Matter* **2002**, *14*, 2717.
[17] J. P. Perdew, K. Burke, M. Ernzerhof, *Phys. Rev. Lett.* **1996**, *77*, 3865.
[18] S. Grimme, *J. Comput. Chem.* **2007**, *27*, 1787.
[19] J. Heyd, G. E. Scuseria, M. Ernzerhof, *J. Chem. Phys.* **2006**, *124*, 219906.

